Crack Growth Processes During IGSCC of Iron

RUSSELL H. JONES
Pacific Northwest Laboratory,[a] P.O. Box 999, Richland, WA 99352, USA

ABSTRACT

Intergranular stress-corrosion cracking (IGSCC) is generally considered to be an active path corrosion process in which crack growth occurs at the atomic level by anodic dissolution. Crack tip chemistry modeling and acoustic emission monitoring of subcritical crack growth have been used to help reveal some of the critical processes involved in IGSCC. Crack tip chemistry modeling suggests that crack wall corrosion rates, crack tip opening displacement, and crack angle are crucial processes in active path stress corrosion. However, these anodic dissolution processes do not appear to be dominant in IGSCC of Fe.

IGSCC occurs along grain boundaries enriched with impurities or with carbide precipitates, both of which can embrittle the grain boundary. Therefore, mechanical fracture along grain boundaries accompanying active path corrosion is a possibility. Acoustic emission (AE) monitoring has been performed on Fe samples undergoing IGSCC to help elucidate whether mechanical fracture accompanied crack growth. Acoustic emission was detected during crack growth and was correlated with mechanical fracture of ligaments or inclusions behind the crack front. Short crack jumps smaller than about 10 μm were not detectable with the acoustic emission technique; therefore, crack extension by mechanical fracture cannot be ruled out.

INTRODUCTION

Stress corrosion occurs only when the local crack tip chemistry supports a corrosion reaction at the crack tip. The local crack tip chemistry is affected by several variables including the bulk solution chemistry far from the crack or crack tip. Transport processes within the crack are controlled by diffusion, migration, and convection. These processes determine the rate at which ions are transported away from the corroding

---

(a) Operated for the U.S. Department of Energy by Battelle Memorial Institute under Contract DE-AC06-76RLO 1830.

crack tip, the crack tip corrosion rate, and also the rate at which anions are transported to the crack tip. The migration of ions to the crack tip that degrade passive film formation is one manner in which the bulk solution chemistry can affect the crack tip chemistry. Other factors such as crack length, crack width and angle, convection from cyclic loading or corrosion currents, and the location of cathodes for anodically dominated SCC or anodes for cathodically dominated SCC are all important in determining the crack tip corrosion rate.

The concept that the crack wall corrosion rate must differ from the crack tip corrosion rate for SCC to occur has been well established. This differential has generally been associated with SCC occurring in the active-to-passive potential regimes where these two conditions could be satisfied simultaneously. The relationship between this corrosion differential and SCC has generally been linked merely to the aspect ratio of the crack, where high wall corrosion rates result in a low aspect ratio and hence a blunted crack or shallow pit and low wall corrosion rates with a high aspect ratio crack. Danielson, *et al.*, (1987) evaluated the effect of variable wall chemistries on the crack wall corrosion rates and also considered the wall corrosion rate effect in terms of the crack tip chemistry rather than the crack aspect ratio. Variable crack wall chemistries resulted from intergranular stress corrosion cracks propagating along either P- or S-enriched grain boundaries in Ni. To determine whether similar anodic processes occur during IGSCC of Fe with P and S enriched grain boundaries was one of the objectives of this research.

A second objective was to evaluate mechanical fracture processes accompanying IGSCC of Fe. Transgranular SCC by film-induced cleavage has been proposed by Newman and Sieradzki (1987) to explain crack extension processes in a variety of materials. In the case of brass, they proposed that a dealloyed layer is the brittle film that induces cleavage in normally ductile brass. In a later analysis, Sieradzki (1987) concluded that the elastic modulus, film-substrate lattice parameter mismatch, film thickness, and interfacial bond strength are the important parameters that determine whether film-induced cleavage will occur. Intergranular SCC involves the propagation of cracks along grain boundaries that either are embrittled with segregated impurities or in which the properties are likely altered by the presence of precipitates, such as carbides in sensitized stainless steel or intermetallics in aluminum alloys. Therefore, the possibility exists that IGSCC occurs by a combination of anodic dissolution and mechanical fracture.

EXPERIMENTAL PROCEDURE

Materials

Iron alloys with P and Mn additions were produced by induction melting electrolytic grade Glidden A104 Fe as reported previously (Jones *et al.*, 1982). The resulting alloys had low S, C, and N, and moderate O concentrations with variable Mn and P as desired. The cast ingot was forged and rolled to produce sample blanks from which compact tension samples for subcritical crack growth measurements were produced. The sample blanks were heat treated according to the schedule shown in Table 1. The grain size of the samples following the listed heat treatments were 130 and 80 μm for the Fe and Fe+0.03 P alloys, respectively, and about 100 μm for the Fe+0.1 P and Fe+0.1 P+0.1 Mn alloys. Compact tension (CT) fracture blanks

Table 1. Summary of grain boundary chemistries of iron alloys

Alloy	S	P	O	N	C	Heat Treatment Time (hr)/Temp (°C)
Fe	0.23	-	0.06	0.25	0.06	0.5/800 + 240/600
Fe+0.03 P	0.25	0.01	0.04	0.29	0.06	0.5/800 + 240/600
Fe+0.1 P	0.07	0.21	0.06	0.16	0.08	1/800 + 500/500
Fe+0.1 Mn+0.1 P	0.01	0.31	0.05	0.25	0.06	4/850 + 500/500
Typical Transgranular surface	<0.01	<0.02	<0.04	0.04	<0.02	
$Q = \lambda(x)\ S_{Fe}/S_x$	0.40	-	2.23	3.36	2.0	

were machined with dimensions W = 44.45 mm, B = 2.54 mm and a = 19.1 mm where W is the sample width, B the sample thickness, and a is the notch depth as measured from the load center line.

Grain boundary compositions were determined from samples removed from the CT fracture samples following subcritical crack growth. These samples were taken from a location away from the subcritical crack growth surface and fractured in situ in the ultrahigh vacuum chamber of a scanning AES with a spatial resolution of 1 μm. The average grain boundary concentrations resulting from analysis of about 15 intergranular surfaces for each Fe alloy are given in Table 1. The grain boundary coverages were determined from the peak height ratios using equation 1 below.

$$\text{coverage} = I_x/I_{Fe} \cdot S_{Fe}/S_x \cdot \lambda(x) \qquad (1)$$

where I_{Fe} is the observed peak-to-peak Auger signal for the 703 eV Fe peak, I_x is the observed peak-to-peak Auger signal for segregated element x, S_x and S_{Fe} are the relative sensitivities for pure bulk materials, and $\lambda(x)$ is the electron escape depth in monolayers. The product of $\lambda(x)$ and S_{Fe}/S_x is given in Table 1 as Q. Adsorption from the AES background gases was determined to be minimal from evaluating the time-dependent change in the AES signal in a specific location on a transgranular surface.

The subcritical crack growth behavior of the Fe alloys in 55% $Ca(NO_3)_2$ was determined using compact tension samples loaded in a three-electrode cell. A platinum counter electrode surrounded the uncracked ligament of the sample and the sample potential was controlled relative to a saturated calomel electrode. The samples were electrically isolated from the test frame with ceramic insulators between the loading pins and sample. One- to

2-mm-long precracks were produced in the samples with a servohydraulic test frame operated at a ΔK of 14 MPa$\sqrt{m}$ and a frequency of 10 Hz before immersion in the calcium nitrate solutions. Subcritical crack growth measurements were made by holding the sample at a constant load for a time interval sufficient to obtain the crack growth rate at the selected stress intensity. The crack length was measured with a linear-variable differential transformer (LVDT) crack opening displacement (COD) gage with a sensitivity of 8×10^{-5} mm of crack mouth opening, and the load was applied with a constant crosshead machine.

Acoustic emission measurements were made during subcritical crack growth for the purpose of assessing the possibility that IGSCC of Fe in calcium nitrate is accompanied by discontinuous crack jumps. Acoustic emission was monitored during crack growth with a PZT-5 element epoxied to a 25-cm-long by 0.3-cm stainless steel wave guide screwed into the top of the sample above the solution level. The AE event threshold was set at 2 dB above the electronic noise level and the sample background noise was subtracted from the data collected during crack growth. The AE event rate and sum of events were obtained as a function of crack length and stress intensity. The sample load and COD data were collected on the data acquisition system.

RESULTS AND DISCUSSION

Grain Boundary Chemistry Effects

Intergranular subcritical crack growth was observed in all the Fe alloys in 55% $Ca(NO_3)_2$ at 60°C. The fracture surfaces were 96% or more intergranular, as shown by the typical fractographs for the Fe+0.03 P and Fe+0.1 P alloys in Fig. 1. The Fe+0.1 Mn+0.1 P alloy, which had the highest grain boundary P concentration, was 100% intergranular. The other alloys exhibited a few percent transgranular fracture. A typical crack velocity-stress intensity curve for the Fe alloys is shown in Fig. 2. The Fe and Fe+0.3 P alloys exhibited more tendency toward stage I and II SCC behavior, but this trend was not observed in each sample tested. However, none of the Fe+0.1 P or Fe+0.1 Mn+0.1 P alloys exhibited stage II cracking.

The stress intensity threshold, K_{ISCC}, was relatively independent of grain boundary chemistry as shown in Fig. 3. Stress intensity thresholds ranging from 3 to 7 MPa$\sqrt{m}$ were observed; the lowest value was associated with a grain boundary P concentration of 0.3 monolayers. There is a slight trend toward decreasing threshold with increasing grain boundary P concentration. Increasing grain boundary P concentrations corresponds to decreasing grain boundary S concentrations because of competitive segregation and addition of Mn to reduce S segregation in the Fe+0.1 Mn+0.1 P alloy. Therefore, it is not possible to conclude unambiguously that increased P segregation caused the decrease in the threshold; however, this is the most likely explanation. A fracture mode of 100% intergranular for the samples with 0.3 monolayers of P segregation further supports the conclusion that K_{ISCC} decreases with increasing P segregation. Values of K_{ISCC} of 7 MPa$\sqrt{m}$ and extensive IGSCC also occurred with 0.23 and 0.25 monolayers of S segregation with relatively no P segregation. Therefore, IGSCC of Fe readily occurs in $Ca(NO_3)_2$ with either P or S segregation.

In previous work on Ni (Danielson *et al.*, 1984), S was not found to cause extensive IGC or IGSCC because of its tendency to remain on the walls of

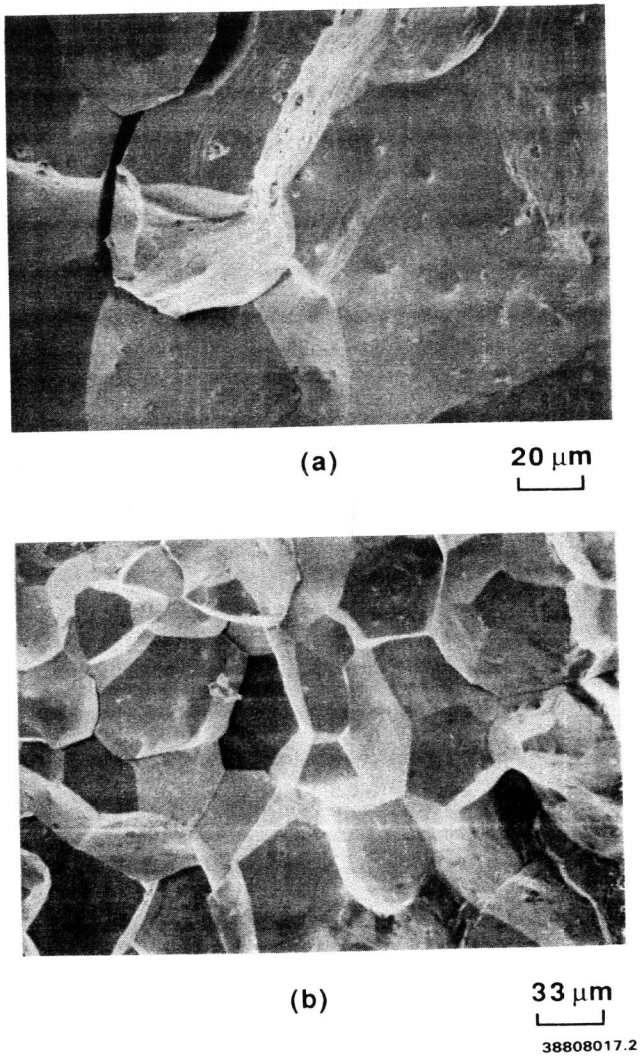

Fig. 1. Scanning electron micrographs of subcritical crack growth surfaces of Fe alloys cracked in 55% $(Ca(NO_3)_2$ at 60°C and +750 mV; a) Fe+0.03 P and b) Fe+0.1 P.

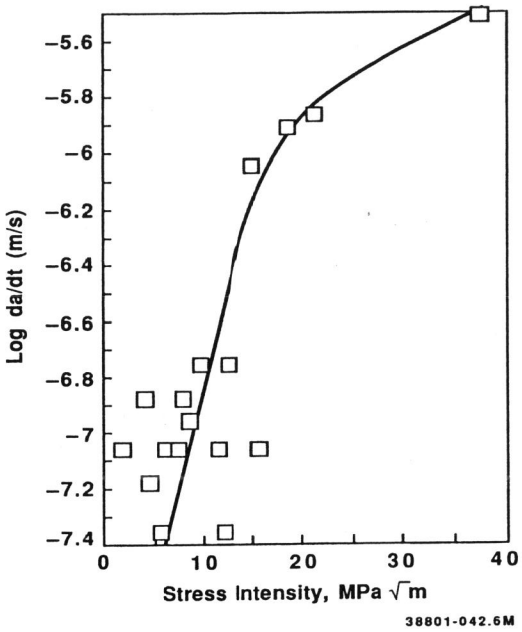

Fig. 2. Crack velocity versus stress intensity for Fe+0.03 P tested in 55% $Ca(NO_3)_2$ at 60°C and +750 mV.

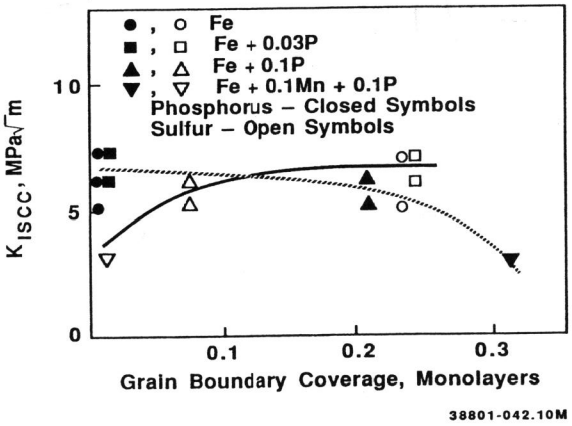

Fig. 3. Threshold stress intensity versus grain broundary P and S concentrations for Fe alloys tested in 55% $Ca(NO_3)_2$ at 60°C and +750 mV.

the grain boundary or crack during IGC or IGSCC, respectively, and to inhibit the formation of the needed active tip/passive wall condition. Phosphorus, on the other hand, did not remain on the wall surfaces and active IGC and IGSCC were observed. Jones *et al.*, (1986) showed that for the conditions of these tests in 1N H_2SO_4, P is oxidized from the grain boundary at the crack tip, leaving the crack walls at the matrix nickel composition and thus allowing passivation to occur. Sulfur is very surface active and remains on the crack walls, which keeps them in he actively corroding condition at potentials in the active-to-passive transition, while sulfur is converted to a sulfate at transpassive potentials, allowing nickel to passivate. Therefore, sulfur-enriched grain boundaries can either result in active walls/active tip or passive walls/passive tip. Using the crack tip chemistry model adapted from Turnbull and Thomas (1982), Danielson, *et al.*, (1984) calculated the effect of the crack wall corrosion rate on the crack tip corrosion rate. Similar concentrations of P and S in the grain boundary would produce similar crack tip corrosion rates based on tests with flat samples doped with P or S. For a 2-mm-long crack at low crack angles, the potential in the crack of the sulfur-enriched intergranular cracks is such that the crack walls are active, which causes nickel sulfate salt precipitation while, as the crack opens to an angle greater than 0.30, the crack walls and crack tip are passive. These crack wall conditions limited the crack tip corrosion rate to 0.065 mA/cm^2 for the sulfur-enriched cracks; a crack tip corrosion rate of 175 mA/cm^2 resulted for a 2-mm-long phosphorus-enriched crack at an angle of about 0.5 deg.

Based on the stress-corrosion tests of Fe with large grain boundary S or P concentrations, there is no evidence for a similarity between the effect of S and P in Ni and Fe. This is somewhat surprising since S exhibits similar segregation behavior in both Ni and Fe and has been found to be strongly bound to the surface of both Ni and Fe (Jones *et al.*).

Acoustic Emission From IGSCC of Fe

Acoustic emission measurements were made during subcritical crack growth of Fe+0.03 P and Fe+0.1 Mn+0.1 P alloys. In these two cases, the most intense AE activity was during the first 1-2 mm of crack extension, with a lower event rate per unit of crack extension for the next 3 mm, as shown in Fig. 4. The number of events per mm of crack extension was 250 and 285 for the Fe+0.03 P and Fe+0.1 Mn+0.1 P alloys, respectively, for the first 1-2 mm of crack extension. The Fe+0.1 Mn+0.1 P alloy exhibited an intermediate event rate of 25 events/mm as a transition between the initially high event rate and the rate observed during the last 3 mm of crack extension. The two alloys exhibited significantly different event rates during the last 3 mm of crack extension, with event rates of 54 and 3 events/mm for the Fe+0.3 P and Fe+0.1 Mn+0.1 P alloys, respectively. Since the stress intensity is increasing with crack extension in these tests, the initial crack extension corresponds to the threshold stress intensity of about 5 MPa√m followed by stages I and II, as shown in Fig. 2. Therefore, the high AE rate corresponds to stage I crack growth, and it has been shown previously (Jones *et al.*, 1984) that most of the plastic zone development occurs in this regime. Therefore, the high AE rate appears to be associated with some process occurring during plastic zone development. This process could be dislocation initiation and multiplication, inclusion fracture or twinning. That the AE activity is lowest when the stress-corrosion crack growth rate is the fastest suggests that the AE source, during the initial crack growth, has ceased and very little AE accompanies crack advance. The number of AE

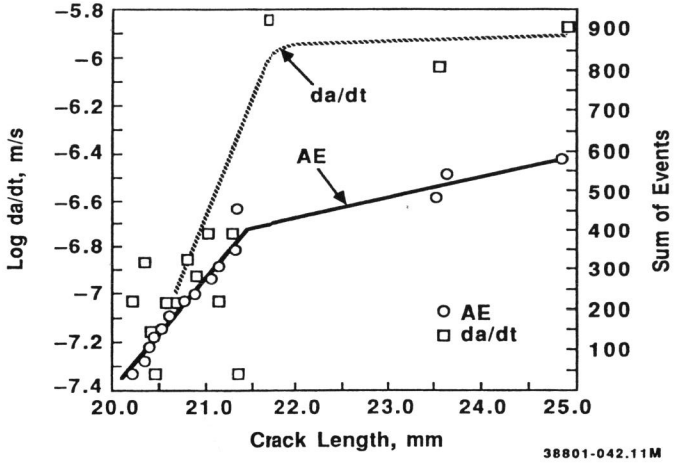

Fig. 4. Crack velocity and total AE events versus crack length for Fe+0.03 P alloy tested in 55% $Ca(NO_3)_2$ at 60°C and +750 mV.

events/mm^2 of IGSCC based on the stage II crack growth regime is shown plotted as a function of the percent transgranular fracture in Fig. 5 along with data for Type 304 SS, Ni + P and a tool steel. A more complete description of these data can be found in Jones *et al*. The data presented in Fig. 5 have been used to conclude that the primary source of AE during stage II crack extension resulted from the fracture of transgranular ligaments behind the advancing crack tip. These ligaments result from the nonuniform crack front caused by nonuniform intergranular corrosion. Intergranular corrosion is nonuniform because of the distribution in segregants such as S and P from grain boundary to grain boundary. The lack of AE from the intergranular crack advance in Fe is underscored by the low AE event rate of about 2 events/mm^2 for the Fe+0.1 Mn+0.1 P alloy, which cracked in a 100% intergranular mode.

Rapid crack acceleration and deceleration is a primary source of AE (Wadley *et al*., 1980) during mechanical fracture of materials. Therefore, the AE results obtained from IGSCC of Fe in $Ca(NO_3)_2$ are not consistent with large crack jumps accompanying an intergranular corrosion process. Likewise, no crack arrest marks have been observed on the intergranular stress-corrosion surfaces although there was an extensive effort to locate them. An estimate of the sensitivity of the AE equipment used in these experiments suggests that crack jumps on the order of about 10 μm or greater should be detectable. Therefore, if mechanical fracture accompanies intergranular corrosion, the crack jumps must be smaller than about 10 μm. An adsorption-type process that causes mechanical fracture at the atomistic level or crack jumps smaller than 10 μm cannot be ruled out by the AE results. Therefore, the possibility of mechanical fracture enhancing the anodic-dissolution-limited crack growth rate must consider processes which could produce short or atomistic crack jumps.

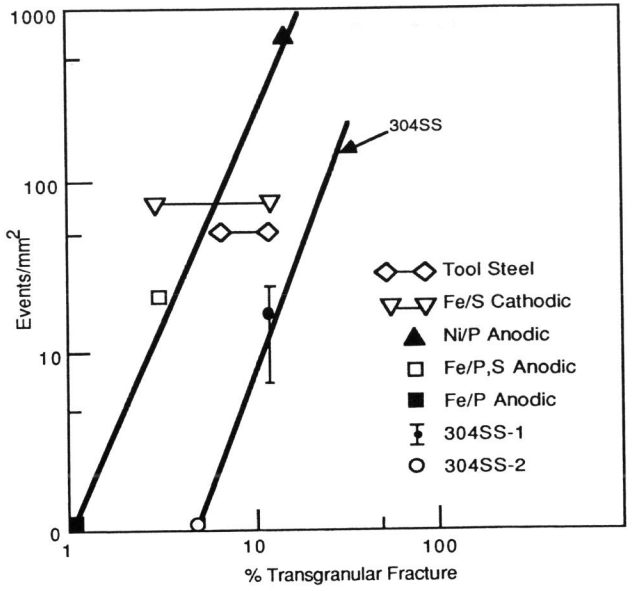

Fig. 5. AE events per mm^2 of fracture surface versus percent transgranular fracture surface for all materials tested.

CONCLUSIONS

The intergranular subcritical crack growth behavior of Fe alloys with S and P segregation has been determined at +750 mV (SCE) in 55% $Ca(NO_3)_2$ at 60°C. IGC and IGSCC occurred with either segregant; there was some evidence that P was slightly more detrimental. This evidence included the increase in the percent intergranular from 96% to 100% and the decreasing stress intensity necessary to produce a crack velocity of 10^{-6} m/s with increasing P segregation. Also, no stage II cracking was observed in the Fe alloys with high P segregation, while some evidence of stage II was observed in the Fe alloys with S segregation.

A stress intensity threshold of about 5 MPa$\sqrt{m}$ was measured for the onset of IGSCC of Fe in $Ca(NO_3)_2$. Crack velocities as high as 10^{-5} m/s were also observed. These crack velocities would require a crack tip corrosion rate of about 20 A/cm^2, which is thought to be unrealistic. Acoustic emission measurements during crack growth do not indicate large (10 μm) intergranular crack jumps but rather the fracture of ligaments behind the crack front. The possibility of atomistic or short jumps of less than 10 μm cannot be ruled out.

REFERENCES

Danielson, M.J., C.A. Oster and R.H. Jones (1984). Corrosion chemistry in intergranular corrosion crack of Nickel containing segregated phosphorus and sulfur. In: *Proceedings of a Conference on Corrosion Chemistry Within Pits, Crevices, and Cracks*. National Physical Laboratory, U.K.

Jones, R.H., S.M. Bruemmer, M.T. Thomas and D.R. Baer (1982). *Metall. Trans. A.*, 13A, p. 241.

Jones, R.H., M.J. Danielson and D.R. Baer (1986). *Journal of Materials for Energy Systems*, 18, p. 185.

Jones, R.H., D.R. Baer, L.A. Charlot and M.T. Thomas (in press). *Metall. Trans.*

Jones, R.H., M.T. Thomas and D.R. Baer (1984). *Scripta Met.*, 18, p. 47.

Jones, R.H., M.A. Friesel and W.W. Gerberich (in press). *Metall. Trans.*

Newman, R.C. and K. Sieradzki (1987). In: *Chemistry and Physics of Fracture*. (R.M. Latanision and R.H. Jones, Eds.) Martinus Nijhoff Publishers, The Netherlands, p. 597.

Sieradzki, K (1986). In: *Proceedings of Modeling Environmental Effects on Crack Growth Processes*. (R.J. Jones and W.W. Gerberich, Eds.) TMS-AIME, Warrendale, PA, pp. 187-196.

Turnbull, A and J.G.N. Thomas (1982). *Journal Electrochemical Society*, 129, 1412-1422.

Wadley, H.N.G., C.B. Scruby and J.H. Speake (1980). *International Metals Reviews*, No. 2 p. 41.